JOC The Journal of Organic Chemistry

Article

pubs.acs.org/joc

Potential Nonadiabatic Reactions: Ring-Opening 4,6-Dimethylidenebicyclo[3.1.0]hex-2-ene Derivatives to Aromatic Reactive Intermediates

Kyle S. Stumetz, Jason T. Nadeau, and Matthew E. Cremeens*

Department of Chemistry and Biochemistry, Gonzaga University, 502 East Boone Avenue, Spokane, Washington 99258, United States

Supporting Information

ABSTRACT: Potential singlet−triplet surface crossings for the ring opening of 4,6-dimethylidenebicyclo[3.1.0]hex-2-ene derivatives were explored using density functional theory (DFT) and complete active space self-consistent field (CASSCF) methods. Since these ring openings involve relatively high energy species that lead to relatively stable aromatic species, a good scenario for potential nonadiabatic events, we posited that the reaction paths of these ring openings might come close to or cross excited state surfaces. At the DFT level of theory, all reaction paths exhibited characteristics suggestive of singlet−triplet intersections along their paths. 6-Methylidenebicyclo[3.1.0]hex-3-en-2-one and a closely related derivative (4-methylidenebicyclo[3.1.0]hex-2-en-6-one) were explored at the CASSCF level of theory; CASSCF results were qualitatively similar to DFT results and yielded spin−orbit couplings of 1.1−1.4 cm^{-1} at the singlet−triplet crossing points.

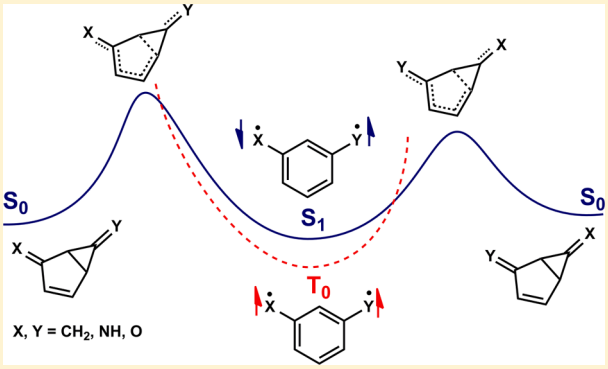

INTRODUCTION

Thermal or nonphotochemical organic reaction mechanisms largely remain on ground-state electronic surfaces and follow the lowest energy pathway: i.e., an adiabatic pathway.[1−7] In what nonphotochemical scenarios ought an organic chemist take seriously the possibility of accessing excited-state electronic surfaces? Carpenter's 2006 review, "Electronically nonadiabatic thermal reactions of organic molecules", provided a platform for the organic chemist to consider this question.[3] Upon going from reactants with paired electrons (closed shell) to intermediates with unpaired electrons (open shell), a crossing of electronic surfaces might take place depending on the energetics. For example, if the closed-shell reactant is high energy and the open-shell intermediate is relatively stable, then a surface crossing might occur along the reaction coordinate if the closed-shell electronic surface of the intermediate is higher in energy than the open-shell surface. Consequently, there is a chance that some fraction of closed-shell molecules remains on the surface that they started on, as opposed to crossing to the lower energy open-shell surface; not following the lowest energy pathway would be a nonadiabatic event leading to an excited-state intermediate.[3,7] We aimed to identify thermal reactions whereby relatively high energy ring-strained molecules ring open to relatively low energy aromatic reactive intermediates and exhibit nonadiabatic events. Our motivation arises partially out of our interest in the topic's potential relevance to combustion chemistry and partially because of our basic scientific curiosity, since few thermal reactions are known to exhibit nonadiabatic behavior. Consequently, in this report we aimed to computationally identify reactions predicted to be capable of undergoing nonadiabatic events during a thermal reaction. Ideally, such reactions could be experimentally tested for nonadiabatic behavior in future experiments.

Derivatives of 4,6-dimethylidenebicyclo[3.1.0]hex-2-ene appeared to be good targets, since they are strained molecules whose ring opening leads to aromatic reactive intermediates (Figure 1).[8−19] The potential surface crossings for these ring openings likely involve singlet and triplet electronic surfaces, because the ring openings start from singlet reactants and lead to diradicals[20] that are predicted to have triplet ground states.[21,22] Additionally, intersystem crossing along the reaction coordinate is expected to be slow;[3,7] consequently, a nonadiabatic event likely occurs such that the singlet excited state is populated before the triplet ground state. The 4,6-dimethylidenebicyclo[3.1.0]hex-2-ene derivatives explored in this study include cases where X and Y are CH_2, NH, or O (Figure 1) for a total of nine permutations. Figure 2 gives the prior computational and/or experimental work found for the ring openings of some derivatives (e.g., X = Y = CH_2,[11,13,19] X = Y = O,[16,17] X = O/Y = CH_2[8−10]); literature reports were not found for the ring opening of the remaining derivatives. Briefly describing some of the prior work for the X = O/Y = CH_2 derivative will help to frame the current efforts. Berson and co-

Received: August 22, 2013
Published: October 14, 2013

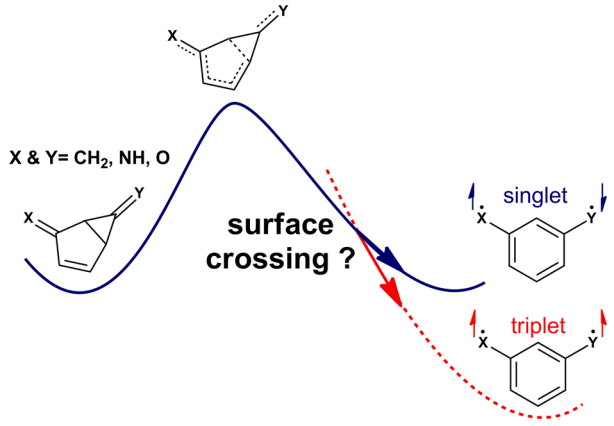

Figure 1. Qualitative depiction of the ring openings of 4,6-dimethylidenebicyclo[3.1.0]hex-2-ene derivatives and their potential nonadiabatic surface crossings.

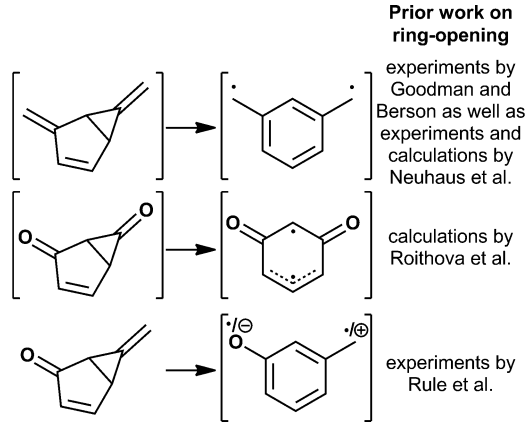

Figure 2. List of prior work on the ring openings of three 4,6-dimethylidenebicyclo[3.1.0]hex-2-ene derivatives (X = Y = CH_2,[13,19] X = Y = O,[16] X = O/Y = CH_2[10]).

workers synthesized and isolated 6-methylidenebicyclo[3.1.0]-hex-3-en-2-one (X = O/Y = CH_2), as well as characterized its reactivity; they observed a triplet diradical via EPR from low-temperature photolysis ethers from thermolysis or photolysis in alcohols, and intractable materials from pyrolysis (150 °C) or photolysis in 4-isoprolytoluene.[8−10] In sum, their experimental work appeared to indicate the presence of both singlet zwitterion and triplet diradical intermediates. However, it was not entirely clear to the authors if the thermal (non-photochemical) reaction path involved singlet−triplet surface crossings or if the singlet zwitterion is similar in energy to the triplet biradical when in an alcoholic solvent. Herein we aim to address the first part of the question: namely, that of singlet−triplet surface crossings. We describe the ring openings for all nine 4,6-dimethylidenebicyclo[3.1.0]hex-2-ene derivatives at the DFT level of theory to identify any qualitative trends and potentially new experimental targets. Additionally, the singlet and triplet surfaces of 6-methylidenebicyclo[3.1.0]hex-3-en-2-one and a related derivative (4-methylidenebicyclo[3.1.0]hex-2-en-6-one)[23] were explored at the DFT and CASSCF levels of theory to evaluate the potential for singlet−triplet surface crossings.

RESULTS AND DISCUSSION

All nine 4,6-dimethylidenebicyclo[3.1.0]hex-2-ene derivatives and their respective ring openings were evaluated at the B3LYP and B3PW91 levels of theory to characterize reaction paths that might give rise to potential singlet−triplet crossings (Figures 3 and 4, Tables 1 and 2). Such crossings should be expected, given that the singlet reactants ring open to diradicals that are predicted to be ground state triplets.[21,22] Using spin-projected singlet energies (see Computational Methods), Table 3 gives their estimated singlet−triplet energy gaps along with available literature values.[24−30] Even though the diradical intermediates were predicted to be triplet ground states, it was not entirely clear whether potential singlet−triplet crossings would take place before or after the transition state. To clarify this matter, triplet states of the transition states were calculated, which were higher in energy than the singlet state and consequently

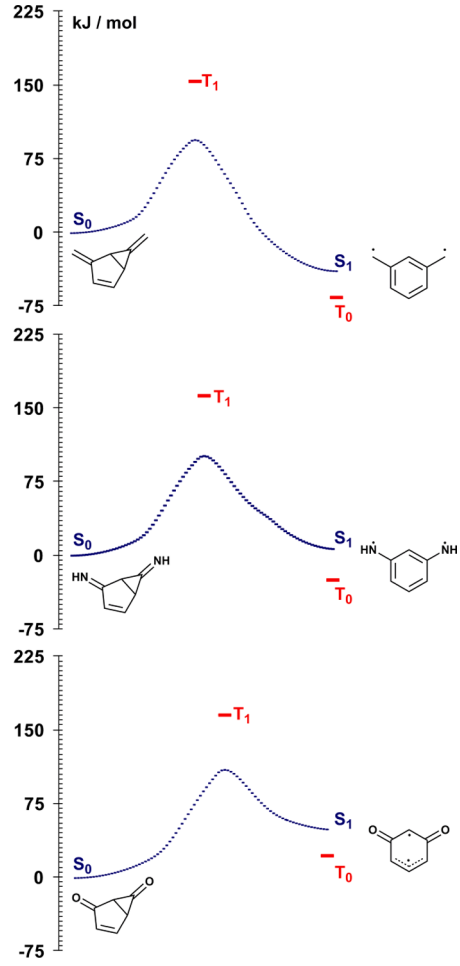

Figure 3. B3PW91 intrinsic reaction coordinates for the singlet surface of the symmetric cases (X = Y). For selected stationary points, a triplet wave function was calculated at a singlet optimized geometry. Although IRCs were calculated with C_1 symmetry, the resulting planar singlet/triplet diradicals exhibited C_{2v} symmetry with $^3B_2$ and $^1B_2$ states for X = Y = O, $^3B_2$ and $^1A_1$ states for X = Y = CH_2, and $^3B_2$ and $^1A_1$ states for X = Y = NH. Different resonance contributors likely better represent different electronic states; only one contributor is shown for simplicity, namely that of the S_1 state. Note that the apparent kink along the X = Y = NH IRC likely results from a nearby singlet surface, presumably that related to the $^1B_2$ state.

dx.doi.org/10.1021/jo401856r | J. Org. Chem. 2013, 78, 10878−10884

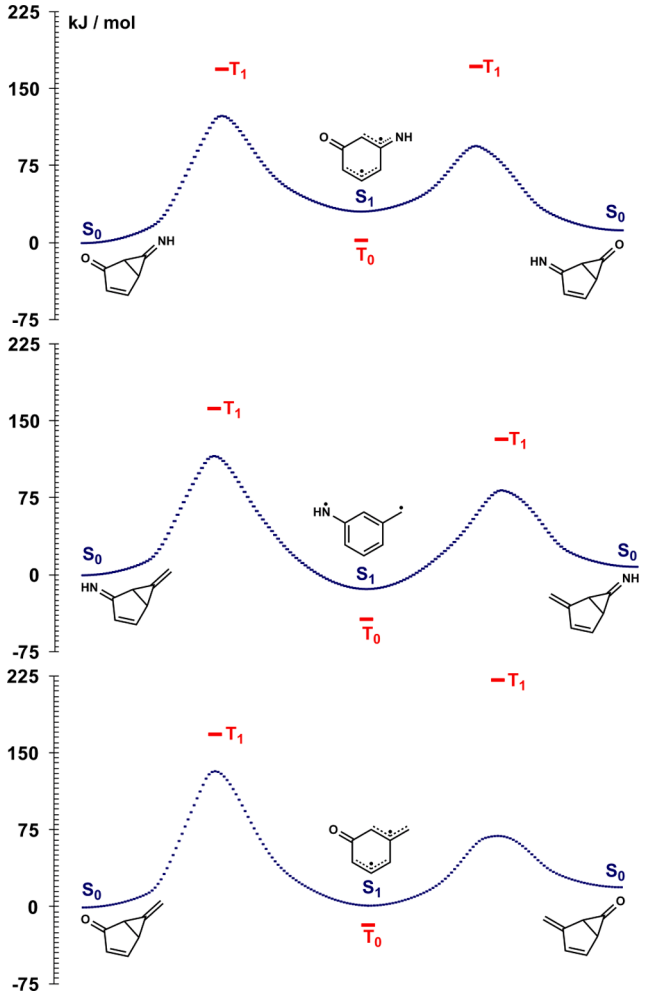

Figure 4. B3PW91 intrinsic reaction coordinates for the singlet surface of the asymmetric cases (X ≠ Y). For selected stationary points, a triplet wave function was calculated at a singlet optimized geometry. Although IRCs were calculated with C_1 symmetry, the resulting planar singlet/triplet diradicals exhibited C_s symmetry with ^{3}A′ and ^{1}A′ states. Different resonance contributors likely better represent different electronic states; only one contributor is shown for simplicity, namely that of the S_1 state.

indicated the potential for post transition state crossings in all nine ring openings (see Figures 3 and 4).

Additionally, the estimated barrier heights for the postulated ring openings at the DFT level of theory provided guidance as to which molecules may or may not be readily isolable in a laboratory. In Figure 3 and Table 1, we report the B3PW91 and B3LYP predictions for the symmetric derivatives (X = Y), which exhibited modest ring-opening barriers (83−110 kJ/mol) and singlet intermediates that went from being exothermic (X = Y = CH_2) to endothermic (X = Y = O) with estimated singlet−triplet energy gaps of 53−63 kJ/mol (Table 3). Note that the predicted change from exothermic to endothermic ring openings of X = Y = CH_2 and X = Y = O likely relates differences in electronic states for their intermediates (see Figure 3), where the $^1A_1$ state for X = Y = CH_2 has more aromatic character than the $^1B_2$ state for X = Y = O. In Figure 4 and Table 2, we report the B3PW91 and B3LYP predictions for the asymmetric cases (X ≠ Y), which also exhibited modest ring-opening barriers (70−133 kJ/mol) and singlet intermediates that went from being exothermic (X, Y = NH, CH_2) to endothermic (X, Y = NH, O) with estimated singlet−triplet energy gaps of 35−60 kJ/mol (Table 3). Note that for the asymmetric cases, when oxygen (i.e., the more electronegative atom) is in the X position, the lower the starting material energy, the higher the barrier height, while the reverse is true when oxygen is in the Y position. This trend is consistent with experimental data for the ring opening of the related ring-strained molecules 2-methylmethylenecyclopropane and *trans*-2,3-di-*tert*-butylcyclopropanone, where the ring-opening barriers are 169 and 118 kJ/mol, respectively.[31,32] When X = O/Y = CH_2, NH, O as well as when X = NH/Y = CH_2, NH, the ring-opening barrier heights are above 100 kJ/mol, while related ring-strained molecules have reported syntheses, e.g. 2-methylmethylenecyclopropane, cyclopropanimine, and cyclopropanone;[31,33,34] consequently, these derivatives can serve as potential synthetic targets (Figure 5). However, the obvious first synthetic target is that of a derivative with a reported synthesis. To the best of the authors' knowledge, only the X = O/Y = CH_2 derivative has been synthesized and isolated,[8−10] which might not be surprising since it is predicted to have the highest ring-opening barrier. Consequently, we focused on the details of the X = O/Y = CH_2 derivative. Since the asymmetric derivatives provide a good system for potentially studying dynamics associated with possible singlet−triplet crossing points, and given that the starting materials have different relative energies and different barrier heights but lead to the same reactive intermediate, we

Table 1. DFT Results for the Stationary Points of the Symmetric Cases (X = Y)[a]

		B3LYP			B3PW91		
X	Y	starting material	transition state	intermediate	starting material	transition state	intermediate
CH_2	CH_2						
singlet (μ, S^2)		0.0 (0.52, 0)	83.2 (1.59, 0.20)	−51.3(0.13, 1.01)	0.0 (0.51, 0)	94.8 (1.54, 0.25)	−38.7 (0.09, 1.01)
triplet (μ, S^2)		299.0 (0.30, 2.00)	147.7 (1.02, 2.08)	−77.6 (0.12, 2.07)	293.4 (0.29, 2.00)	154.4 (1.01, 2.09)	−65.7 (0.09, 2.07)
NH	NH						
singlet (μ, S^2)		0.0 (1.92, 0)	88.6 (1.61, 0.25)	−11.3 (0.03, 0.97)	0.0 (1.96, 0)	101.5 (1.59, 0.31)	6.6 (0.11, 0.98)
triplet (μ, S^2)		324.8 (1.80, 2.01)	154.0 (1.41, 2.06)	−40.9 (0.54, 2.07)	321.5 (1.83, 2.01)	162.6 (1.45, 2.07)	−25.0 (0.60, 2.08)
O	O						
singlet (μ, S^2)		0.0 (3.86, 0)	96.0 (3.88, 0.33)	45.1 (3.81, 0.95)	0.0 (3.89, 0)	110.2 (3.86, 0.40)	67.1 (3.80, 0.96)
triplet (μ, S^2)		329.1 (3.50, 2.01)	155.2 (3.57, 2.04)	4.2 (3.07, 2.06)	328.2 (3.52, 2.01)	165.8 (3.60, 2.04)	22.5 (3.07, 2.07)

[a]Electronic energies (kJ/mol) relative to starting material are presented with dipoles (debye) and S^2 values in parentheses. Triplet data come from triplet optimized wavefunctions for singlet optimized geometries. Absolute energies (hartree) and Cartesian coordinates are given in the Supporting Information.

dx.doi.org/10.1021/jo401856r | J. Org. Chem. 2013, 78, 10878−10884

Table 2. DFT Results for the Stationary Points of the Asymmetric Cases (X ≠ Y)[a]

		B3LYP			B3PW91		
X	Y	starting material	transition state	intermediate	starting material	transition state	intermediate
O	CH_2						
singlet (μ, S^2)		0.0 (3.53, 0)	121.3 (3.30, 0.53)	−14.6 (4.99, 0.85)	0.0 (3.56, 0)	132.7 (3.33, 0.57)	1.7 (4.96, 0.87)
triplet (μ, S^2)		307.6 (1.93, 2.01)	159.7 (4.16, 2.05)	−31.9 (3.58, 2.06)	305.2 (1.92, 2.01)	168.5 (4.18, 2.05)	−17.4 (3.60, 2.07)
CH_2	O						
singlet (μ, S^2)		19.8 (2.54, 0)	58.7 (4.19, 0)	same as above	19.7 (2.53, 0)	69.7 (4.46, 0)	same as above
triplet (μ, S^2)		310.9 (3.43, 2.03)	243.2 (2.90, 2.05)		307.7 (3.43, 2.03)	221.4 (2.97, 2.07)	
NH	CH_2						
singlet (μ, S^2)		0.0 (2.67, 0)	104.6 (1.95, 0.39)	−28.5 (2.51, 0.99)	0.0 (2.71, 0)	116.2 (2.02, 0.44)	−13.4 (2.53, 1.00)
triplet (μ, S^2)		328.2 (2.47, 2.01)	154.4 (3.28, 2.06)	−56.8 (2.41, 2.07)	323.9 (2.50, 2.01)	162.3 (3.30, 2.07)	−43.1 (2.45, 2.08)
CH_2	NH						
singlet (μ, S^2)		8.4 (1.73, 0)	70.2 (4.02, 0.01)	same as above	8.3 (1.73, 0)	82.9 (3.98, 0.08)	same as above
triplet (μ, S^2)		302.4 (1.74, 2.00)	156.0 (1.71, 2.07)		296.8 (1.78, 2.00)	132.4 (1.87, 2.09)	
O	NH						
singlet (μ, S^2)		0.0 (2.30, 0)	111.2 (2.11, 0.44)	12.5 (2.38, 0.94)	0.0 (2.31, 0)	124.0 (2.09, 0.50)	30.7 (2.32, 0.95)
triplet (μ, S^2)		313.5 (1.18, 2.01)	159.5 (2.11, 0.44)	−14.4 (1.50, 2.06)	311.7 (1.18, 2.01)	169.3 (2.09, 2.05)	2.5 (1.47, 2.07)
NH	O						
singlet (μ, S^2)		12.5 (2.85, 0)	80.5 (2.84, 0.07)	same as above	12.5 (2.89, 0)	94.7 (2.79, 0.15)	same as above
triplet (μ, S^2)		322.5 (2.59, 2.02)	162.9 (2.03, 2.05)		320.8 (2.61, 2.02)	171.9 (2.03, 2.06)	

[a]Electronic energies (kJ/mol) relative to starting material are presented with dipoles (debye) and S^2 values in parentheses. Triplet data come from triplet optimized wavefunctions with singlet optimized geometries. Absolute energies (hartree) and Cartesian coordinates are given in the Supporting Information.

Table 3. DFT Singlet−Triplet Energy Gaps ($\Delta E_{S\text{-}T} = E_S - E_T$) in kJ/mol[a]

X	Y	B3LYP	B3PW91	lit.
CH_2	CH_2	53	55	40.2 ± 0.8 (experiment[24])
NH	NH	59	63	66.1 (UB3LYP/6-311+G(d,p)[25])
O	O	60	59	49.8 (CASPT2N/6-31G(d)[27])
O, CH_2	CH_2, O	35	38	38.9 (CASPT2N/6-31G(d)[27])
NH, CH_2	CH_2, NH	57	60	78 (AM1-CI[29])
O, NH	NH, O	53	56	n.d.

[a]Singlet and triplet energies were from singlet and triplet geometry optimizations, respectively. $\Delta E_{S\text{-}T}$ values incorporate a spin-projected correction to the singlet energy. No data (n.d.) were found for one case. Experimental values are presented when possible. Experiments are reported for the X = Y = O derivative; however, the spectral analysis is not yet complete.[28]

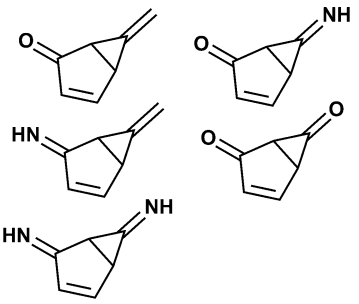

Figure 5. Potential synthetic targets for future experimental work: 4,6-dimethylidenebicyclo[3.1.0]hex-2-ene derivatives with DFT predicted ring-opening barriers of over 100 kJ/mol with the following order: O/CH_2 > O/NH > NH/CH_2 > O/O > NH/NH.

also evaluated the X = CH_2/Y = O derivative, despite it having the lowest ring-opening barrier.

With narrowed targets (X = O/Y = CH_2 and X = CH_2/Y = O), (1) we used the CASSCF method to check the qualitative accuracy of the DFT results, (2) we identified the singlet−triplet crossing points, and (3) we calculated the spin−orbit coupling at the crossing points. For all three methods, the ring-opening barrier for X = O/Y = CH_2 (100−133 kJ/mol) was predicted to be larger than that for X = CH_2/Y = O (39−50 kJ/mol), Table 4, and Figure 6 illustrate the qualitatively similar reaction paths between the DFT and CASSCF methods. For

Table 4. Selected Data for the Crossing Points (CP) and Transition States (TS)

method	TS (kJ/mol)	$CP_{S/T}$ − TS (kJ/mol)	% along IRC from TS	rupturing C−C (Å)
X = O, Y = CH_2				
B3LYP	121	−19	10	2.23
B3PW91	133	−9.5	7.8	2.21
CASSCF	100	−1.5	5.5	2.31
X = CH_2, Y = O				
B3LYP	38.8	−44	44	2.39
B3PW91	50.0	−39	38	2.38
CASSCF	42.4	−25	43	2.37

reference, at the CASSCF level, the S_2 state is predicted to be 106 kJ/mol above the S_1 state and 19 kJ/mol above the transition state, which makes it energetically inaccessible; however, the ring opening of the X = Y = CH_2 derivative might yield an accessible S_2 state, since it was predicted to only be 55 kJ/mol above the S_1 state.[27] Calculated triplet states for singlet geometries along the IRCs at the B3LYP, B3PW91, and CASSCF levels of theory for both X = O/Y = CH_2 and X =

dx.doi.org/10.1021/jo401856r | J. Org. Chem. 2013, 78, 10878−10884

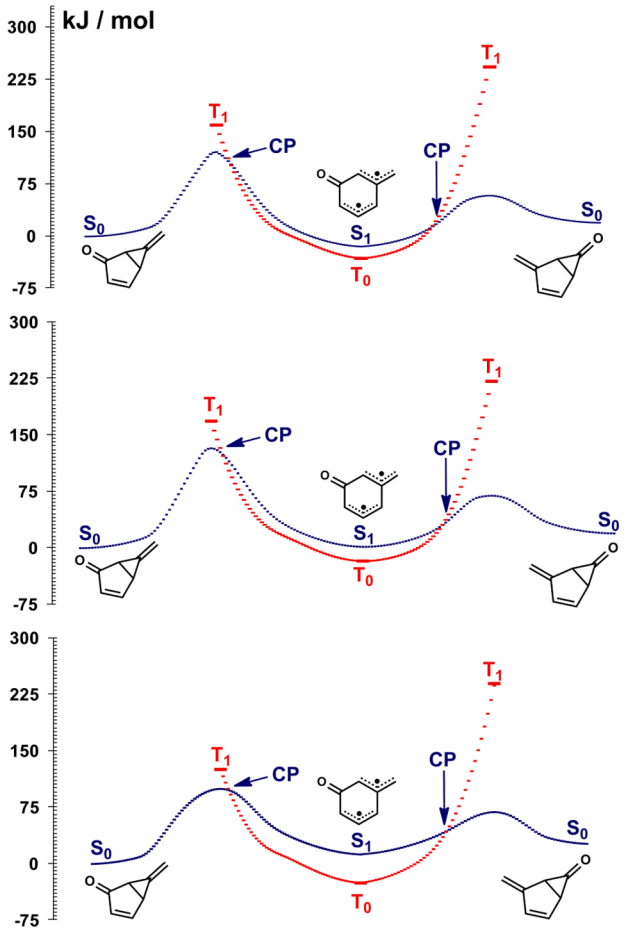

Figure 6. Intrinsic reaction coordinates at the B3LYP (top), B3PW91 (middle), and CASSCF (bottom) levels of theory for the singlet surface (blue) of the asymmetric derivatives (X = O/Y = CH_2; X = CH_2/Y = O). Triplet wave functions were calculated at singlet optimized geometries (red). Different resonance contributors likely better represent different electronic states; only one contributor is shown for simplicity, namely that of the S_1 state.

CH_2/Y = O ring-opening reactions were again qualitatively very similar (Figure 6). Figure 7 overlays the resulting crossing point

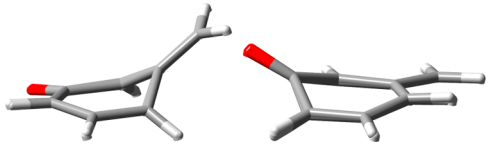

Figure 7. Overlay of B3LYP, B3PW91, and CASSCF crossing point geometries: (left) CP of X = O/Y = CH_2; (right) CP of X = CH_2/Y = O.

structures, which appear to be extremely similar for the three different levels of theory. Note that Harvey and co-workers also found that crossing point geometries are not significantly affected by the level of theory.[35,36] Also note that there is a possibility of an off-path but nearby and potentially lower energy crossing point. The relative crossing point energies (relative to their nearby transition states) are below their nearby transition state and vary up to 19 kJ/mol. In line with geometries being more similar than energies, the percent traveled along the reaction coordinate from the transition state to intermediate varied to a smaller extent, 5.5−10% for X = O/Y = CH_2 and 38−44% for X = CH_2/Y = O, for the DFT and CASSCF levels of theory (Table 4). Given the remarkable similarities between the crossing point structures and the percent traveled along the reaction coordinate, the potential for crossing was explored at the CASSCF level of theory.

To evaluate the potential for crossing from the singlet surface to the triplet surface at the crossing point along the reaction coordinate, the spin−orbit coupling must be evaluated.[37,38] From Turro, Ramamurthy, and Scaiano, spin−orbit coupling is expected to be the primary mechanism for intersystem crossing when the distance between radical centers is <5 Å;[39] for the crossing points in Figure 7, the distance between the carbons of the rupturing C−C bond is 2.2−2.4 Å. At the CASSCF(8,8) level of theory, spin−orbit couplings for the X = O/Y = CH_2 and the X = CH_2/Y = O crossing points were 1.4 and 1.1 cm^{-1}, respectively; the rupturing C−C bond distances were 2.31 and 2.37 Å, respectively. Although the magnitude of this coupling is not exceptionally large, it is not necessarily insignificant; for organic diradicals, a coupling value above 0.1 cm^{-1} might be considered large.[40] For reference, Andrés and co-workers recently calculated a spin−orbit coupling of 4.76 cm^{-1} for a singlet−triplet crossing point along a different ring-opening path.[41] However, an estimation of the transmission probability between the two states is approximately 3.6×10^{-5} (see Computational Methods) and, since a crossing rate on the femtosecond time scale would likely be necessary to compete with remaining on the singlet surface, transition *along* the reaction coordinate to the triplet state seems unlikely.[7] For reference, Schmidt et al. reported on the photophysical properties of monoaza[5]helicenes; in one example where the spin−orbit coupling was calculated to be 12 cm^{-1}, the calculated intersystem crossing rate was 2×10^9 s^{-1}.[42] Consequently, population of the S_1 excited state is expected in the present case and therefore a nonadiabatic transition is expected.

In summary, we have identified that the ring opening of 4,6-dimethylidenebicyclo[3.1.0]hex-2-ene derivatives have post transition state singlet−triplet crossings but likely remain on the singlet surface to yield a nonadiabatic event. For future experimental work, five derivatives were identified as potential synthetic targets (Figure 5), while the most likely target (X = O/Y = CH_2) was explored in greater detail along with a closely related derivative, X = CH_2/Y = O. For these derivatives, both DFT and CASSCF reaction paths were qualitatively similar to similar crossing point geometries, where modest spin−orbit couplings were predicted for the crossing points. Although we have addressed the main point of this work, namely the nonadiabatic nature of these ring openings, a few closing remarks with respect to the potential for experimentally testing these predictions are warranted.

Experimentally evaluating the ring opening and the resulting intermediates could come about in at least two ways. First, the singlet and triplet intermediates for X = O/Y = CH_2 are predicted to have different CO stretching frequencies by approximately 120 cm^{-1} (DFT results: S_1 ν_{CO} ~1575 cm^{-1}, T_0 ν_{CO} ~1455 cm^{-1}, see the Supporting Information). Consequently, IR spectroscopy might provide some insight into whether one or both intermediates are generated. More specifically, matrix isolation and IR analysis of flash vacuum pyrolysis products should work for studying the X = O/Y = CH_2 derivative, since it was used by Sander and co-workers for the X = Y = CH_2 derivative.[19] An alternative approach could build off of the work of Berson and co-workers, whose

dx.doi.org/10.1021/jo401856r | J. Org. Chem. 2013, 78, 10878−10884

experimental results for the X = O/Y = CH_2 derivative indicated both triplet diradical and singlet zwitterion intermediates.[10] Note that the gas-phase calculations reported here and elsewhere for the X = O/Y = CH_2 derivative[27] indicate that the S_1 state is diradical-like. For example, we observed CASSCF occupation numbers of 1.4 and 0.6 for the singly occupied molecular orbitals of the S_1 state (1.0 and 1.0 for T_0). However, when the S_1 state was optimized with an implicit solvent model for either water or methanol, the occupation numbers changed to 1.6 and 0.4 (1.0 and 1.0 for T_0), while the CASSCF $\Delta E_{S\text{-}T}$ value decreased from 49 to 31 kJ/mol. The change in occupation numbers for the S_1 state implies that it might be zwitterionic in a polar environment, like that of an alcohol solvent in the Rule et al. experiments. Consequently, for a given set of reaction conditions, the detection of trapping products derived from both a singlet zwitterion and a triplet diradical could possibly indicate a nonadiabatic event in the ring opening of the X = O/Y = CH_2 derivative; more specifically, the singlet reactant could ring open to an excited state singlet intermediate, which could then undergo intersystem crossing to a triplet ground state.

COMPUTATIONAL METHODS

Using Gaussian09,[43] all ring-opening reactions were computationally characterized with density functional theory (DFT). Intrinsic reaction coordinates (IRC)[44] of the singlet surface were calculated with the B3LYP[45−47] and B3PW91[48] hybrid functionals using the unrestricted, broken spin symmetry approach;[49] some wave functions required the quadratically convergent method[50] or using a triplet wave function as a guess for the singlet diradical wave function. Expected S^2 values for singlet biradicals using a single reference method should be 1.[22] Diradical singlets not only exhibited S^2 values close to 1 but also exhibited dipole moments that were very similar to those of the corresponding triplet state of the singlet optimized geometry. Similar to observations by Hess, potentially zwitterionic singlets exhibited S^2 values less than 0.9 and exhibited increases in dipole moments by over 1 D in comparison to the corresponding triplet state.[51] The use of single-reference DFT for the characterization of singlet diradical surfaces is not without complication;[52,53] hence, the use of CASSCF. Additionally, to check for grotesque errors with the use of DFT for some of these diradical intermediates, an isodesmic reaction[54] was used to compare experimental and DFT values. The heats of formation for the triplet intermediates of X = CH_2/Y = CH_2, X = O/Y = O, and X = CH_2/Y = O have been reported.[55−58] For the following isodesmic reaction using diradical intermediates, X = CH_2/Y = CH_2 + X = O/Y = O → X = CH_2/Y = O + X = O/Y = CH_2, the DFT heat of reaction (−2.4 kcal/mol) falls within the experimental estimate (−8.3 ± 6.5 kcal/mol). Single-reference DFT methods can be used to estimate singlet−triplet energy gaps, but not without spin-projected corrections and an understanding of the associated error.[59−62] Others have developed DFT functionals for improving the accuracy of DFT predicted singlet−triplet energy gaps;[61,62] however, the work here is qualitative and is not limited to singlet−triplet energy gaps. With respect to DFT singlet−triplet energy gaps, spin-projected singlet energies were computed using the Yamaguchi procedure,[63] also found in ref 61: E_S(spin-projected) = $E_S + \chi[E_S - E_T]$, where $\chi = [S^2_S/S^2_T]/[1 - (S^2_S/S^2_T)]$ and the E_T and S^2_T values arise from a triplet optimized wave function of the singlet optimized geometry. For reference, the Noodleman semiempirical correction ($\Delta E_{S\text{-}T} = [E_S - E_T]2/[S^2_S - S^2_T]$)[64,65] yields $\Delta E_{S\text{-}T}$ values that are less than the Yamaguchi correction by 3−6 kJ/mol. To identify singlet−triplet crossing points, triplet wave functions were evaluated using singlet optimized geometries from the singlet IRC. The point at which the singlet and triplet states were approximately isoenergetic (<2 kJ/mol for DFT and <0.25 kJ/mol for CASSCF) was taken as a crossing point. The CASSCF level of theory was used for the X = CH_2/Y = O and X = O/Y = CH_2 derivatives.[66] An eight-electron, eight-orbital active space was selected: i.e., CASSCF(8,8). The reactant active space used all six π/π^* orbitals and the two σ/σ^* orbitals of the rupturing C−C bond; ring opening led to eight π/π^* orbitals for the intermediate. IRCs were calculated under C_1 symmetry. For X = O/Y = CH_2 or X = CH_2/Y = O at the DFT and CASSCF levels, both singlet and triplet intermediates were A′. To be sure that the triplet was ^{3}A′ and not ^{3}A″, the lone pair of electrons on the oxygen in the molecular plane was included in the active space (CASSCF(10,9)), to explore the possibility of a ^{3}A″ state result; ^{3}A′ was lower in energy. To qualitatively survey all of the reactions, studies were completed with the inexpensive 6-31G(d) basis set.[67] Spin−orbit coupling was computed at the CASSCF level of theory,[68] which was reported to exhibit errors of approximately 30%.[69] Electronic energies are reported. Harmonic vibrational frequencies were calculated for all DFT and CASSCF stationary points. CASSCF occupation numbers were taken from the diagonal of the final one-electron density matrix. The inclusion of implicit solvent effects employed the integral equation formalism/polarizable continuum model (IEFPCM) coupled with Truhlar's SMD model.[70] For reference, the S_2 wave function of the X = O/Y = CH_2 intermediate was optimized at the S_1 optimized geometry with the aforementioned (8,8) and (10,9) active spaces; both calculations produced an A′ state with occupation numbers of 1.1 and 0.9 for the singly occupied orbitals. Estimation of the singlet−triplet transition probability arose from the work of German et al.,[71] which relied on the efforts of Kuznetzov.[72,73] According to German et al., the transmission coefficient (κ) between the singlet and triplet states can be approximated as $\kappa \approx [V_{ts}/V_{cr}]^2$, where V_{ts} is the matrix element of the spin−orbit coupling and V_{cr} is its critical value, which can be approximated as k_BT, or 208 cm^{-1} at 298 K. Consequently, κ could be estimated to be $(1.1/208)^2$ to $(1.4/208)^2$ or approximately $(2.8\text{−}4.5) \times 10^{-5}$ for the crossing points in this work.

ASSOCIATED CONTENT

Supporting Information

Tables giving Cartesian coordinates and absolute electronic energies (hartrees). This material is available free of charge via the Internet at http://pubs.acs.org.

AUTHOR INFORMATION

Corresponding Author

*E-mail for M.E.C.: cremeens@gonzaga.edu.

Notes

The authors declare no competing financial interest.

ACKNOWLEDGMENTS

M.E.C. thanks W. T. Borden for a helpful discussion and useful comments, B. K. Carpenter for a helpful discussion and helpful suggestions, and P. G. Wenthold for a helpful discussion. M.E.C. also thanks F. R. Clemente, G. Gidofalvi, and B. Hendricks. M.E.C., K.S.S., and J.T.N. thank the reviewers for helpful comments and suggestions. This research was supported in part by the Gonzaga Science Research Program, Gonzaga University Start-up Funds, and the Gonzaga University Department of Chemistry and Biochemistry.

REFERENCES

(1) Bernardi, F.; Robb, M. A.; Olivucci, M. *Chem. Soc. Rev.* **1996**, *25*, 321−328.
(2) Nikitin, E. E. *Annu. Rev. Phys. Chem.* **1999**, *50*, 1−21.
(3) Carpenter, B. K. *Chem. Soc. Rev.* **2006**, *35*, 736−747.
(4) Mahapatra, S. *Acc. Chem. Res.* **2009**, *42*, 1004−1015.
(5) Bhattacharya, A.; Guo, Y. Q.; Bernstein, E. R. *Acc. Chem. Res.* **2010**, *43*, 1476−1485.
(6) Yarkony, D. R. *Chem. Rev.* **2012**, *112*, 481−498.
(7) Carpenter, B. K. *Chem. Rev.* **2013**, *113*, 7265−7286.

(8) Rule, M.; Matlin, A. R.; Hilinski, E. F.; Dougherty, D. A.; Berson, J. A. *J. Am. Chem. Soc.* **1979**, *101*, 5098−5099.
(9) Seeger, D. E.; Hilinski, E. F.; Berson, J. A. *J. Am. Chem. Soc.* **1981**, *103*, 720−721.
(10) Rule, M.; Matlin, A. R.; Seeger, D. E.; Hilinski, E. F.; Dougherty, D. A.; Berson, J. A. *Tetrahedron* **1982**, *38*, 787−798.
(11) Goodman, J. L.; Berson, J. A. *J. Am. Chem. Soc.* **1984**, *106*, 1867−1868.
(12) Goodman, J. L.; Peters, K. S.; Lahti, P. M.; Berson, J. A. *J. Am. Chem. Soc.* **1985**, *107*, 276−277.
(13) Goodman, J. L.; Berson, J. A. *J. Am. Chem. Soc.* **1985**, *107*, 5409−5424.
(14) Khan, M. I.; Goodman, J. L. *J. Am. Chem. Soc.* **1994**, *116*, 10342−10343.
(15) Itoh, T.; Matsumura, Y.; Kubo, M. *J. Polym. Sci., Part A: Polym. Chem.* **1997**, *35*, 741−746.
(16) Roithova, J.; Schroder, D.; Schwarz, H. *Angew. Chem., Int. Ed.* **2005**, *44*, 3092−3096.
(17) Roithova, J.; Schroder, D.; Schwarz, H. *Chem. Eur. J.* **2005**, *11*, 628−638.
(18) Shurygina, M. P.; Kurskii, Yu. A.; Druzhkov, N. O.; Chesnokov, S. A.; Abakumova, L. G.; Fukin, G. K.; Abakumov, G. A. *Tetrahedron* **2008**, *64*, 9784−9788.
(19) Neuhaus, P.; Grote, D.; Sander, W. *J. Am. Chem. Soc.* **2008**, *130*, 2993−3000.
(20) Abe, M. Diradicals. *Chem. Rev.* **2013**, *113*, 7011−7088.
(21) Borden, W. T.; Davidson, E. R. *J. Am. Chem. Soc.* **1977**, *99*, 4587−4594.
(22) Lineberger, W. C.; Borden, W. T. *Phys. Chem. Chem. Phys.* **2011**, *13*, 11792−11813.
(23) Da Silva, G.; Bozzelli, J. W. *J. Phys. Chem. A* **2007**, *111*, 7987−7994.
(24) Wenthold, P. G.; Kim, J. B.; Lineberger, W. C. *J. Am. Chem. Soc.* **1997**, *119*, 1354−1359.
(25) Rajca, A.; Olankitwanit, A.; Rajca, S. *J. Am. Chem. Soc.* **2011**, *133*, 4750−4753.
(26) Fort, R. C.; Getty, S. J.; Hrovat, D. A.; Lahti, P. M.; Borden, W. T. *J. Am. Chem. Soc.* **1992**, *114*, 7549−7552.
(27) Hrovat, D. A.; Murcko, M. A.; Lahti, P. M.; Borden, W. T. *J. Chem. Soc., Perkin Trans. 2* **1998**, 1037−1044.
(28) Fu, Q.; Yang, J.; Wang, X. B. *J. Phys. Chem. A* **2011**, *115*, 3201−3207.
(29) Zhang, J. P.; Lahti, P. M.; Wang, R. S.; Baumgarten, M. *Heteroat. Chem.* **1998**, *9*, 161−167.
(30) Zhang, J. P.; Yang, G. H.; Wang, R. S.; Wang, L. X. *Chem. Res. Chin. Univ.* **1999**, *15*, 337−342.
(31) Chesick, J. P. *J. Am. Chem. Soc.* **1963**, *85*, 2720−2723.
(32) Sclove, D. B.; Pazos, J. F.; Camp, R. L.; Greene, F. D. *J. Am. Chem. Soc.* **1970**, *92*, 7488.
(33) Quast, H.; Schmitt, E.; Frank, R. *Angew. Chem., Int. Ed. Engl.* **1971**, *10*, 651−652.
(34) Schaafsma, S. E.; Steinberg, H.; DeBoer, T. J. *Rec. Trav. Chim.* **1966**, *85*, 1170−1172.
(35) Harvey, J. N.; Aschi, M.; Schwarz, H.; Koch, W. *Theor. Chem. Acc.* **1998**, *99*, 95−99.
(36) Harvey, J. N. *Phys. Chem. Chem. Phys.* **2007**, *9*, 331−343.
(37) Fedorova, D. G.; Kosekib, S.; Schmidt, M. W.; Gordon, M. S. *Int. Rev. Phys. Chem.* **2003**, *22*, 551−592.
(38) Marian, C. M. Spin-orbit coupling and intersystem crossing in molecules. *WIREs Comput. Mol. Sci.* **2012**, *2*, 187−203.
(39) Turro, N. J.; Ramamurthy, V.; Scaiano, J. C. *Modern Molecular Photochemistry of Organic Molecules*; University Science Books: Sausalito, CA, 2010.
(40) Klessinger, M.; Michl, J. *Excited State and Photochemistry of Organic Molecules*; VCH: New York, 1995.
(41) González-Navarrete, P.; Coto, P. B.; Polo, V.; Andrés, J. *Phys. Chem. Chem. Phys.* **2009**, *11*, 7189−7196.
(42) Schmidt, K.; Brovelli, S.; Coropceanu, V.; Beljonne, D.; Cornil, J.; Bazzini, C.; Caronna, T.; Tubino, R.; Meinardi, F.; Shuai, Z.; Brédas, J. L. *J. Phys. Chem. A* **2007**, *111*, 10490−10499.
(43) Frisch, M. J.; et al. *Gaussian 09, revsion B.01*; Gaussian, Inc., Wallingford, CT, 2010.
(44) Hratchian, H. P.; Schlegel, H. B. *J. Chem. Theory Comput.* **2005**, *1*, 61−69.
(45) Becke, A. D. *J. Chem. Phys.* **1993**, *98*, 5648−5652.
(46) Miehlich, B.; Savin, A.; Stoll, H.; Preuss, H. *Chem. Phys. Lett.* **1989**, *157*, 200−206.
(47) Kruse, H.; Goerigk, L.; Grimme, S. *J. Org. Chem.* **2012**, *77*, 10824−10834.
(48) Perdew, J. P.; Burke, K.; Wang, Y. *Phys. Rev. B* **1996**, *54*, 16533−16539.
(49) Grafenstein, J.; Cremer, D. *Phys. Chem. Chem. Phys.* **2000**, *2*, 2091−2103.
(50) Bacskay, G. B. *Chem. Phys.* **1981**, *61*, 385−404.
(51) Hess, B. A. *J. Am. Chem. Soc.* **2001**, *124*, 920−921.
(52) Bally, T.; Borden, W. T. Calculations on open-shell molecules: a beginner's guide. In *Reviews in Computational Chemistry*; Lipkowitz, K. B., Boyd, D. B., Eds.; Wiley-VCH: New York, 1999; Vol. *13*.
(53) Cremer, D. *Mol. Phys.* **2001**, *99*, 1899−1940.
(54) Wheeler, S. E.; Houk, K. N.; Schleyer, P. v. R.; Allen, W. D. *J. Am. Chem. Soc.* **2009**, *131*, 2547−2560.
(55) Pollack, S. K.; Raine, B. C.; Hehre, W. J. *J. Am. Chem. Soc.* **1981**, *103*, 6308−6313.
(56) Hammad, L. A.; Wenthold, P. G. *J. Am. Chem. Soc.* **2000**, *122*, 11203−11211.
(57) Chacko, S. A.; Wenthold, P. G. *Int. J. Mass Spectrom.* **2007**, *267*, 277−283.
(58) Fattahi, A.; Kass, S. R.; Liebman, J. F.; Matos, M. A. R.; Miranda, M. S.; Morais, V. M. F. *J. Am. Chem. Soc.* **2005**, *127*, 6116−6122.
(59) Hanway, P. J.; Winter, A. H. *J. Am. Chem. Soc.* **2011**, *133*, 5086−5093.
(60) Ess, D. H.; Johnson, E. R.; Hu, X.; Yang, W. *J. Phys. Chem. A* **2011**, *115*, 76−83.
(61) Ess, D. H.; Cook, T. C. *J. Phys. Chem. A* **2012**, *116*, 4922−4929.
(62) Rivero, P.; Jiménez-Hoyos, C. A.; Scuseria, G. E. *J. Phys. Chem. A* **2013**, *117*, 8073−8080.
(63) Onishi, T.; Yamaki, D.; Yamaguchi, K.; Takano, Y. *J. Chem. Phys.* **2003**, *118*, 9747−9761.
(64) Noodleman, L. *J. Chem. Phys.* **1981**, *74*, 5737−5743.
(65) Noodleman, L.; Davidson, E. R. *Chem. Phys.* **1987**, *109*, 131−143.
(66) Yamamoto, N.; Vreven, T.; Robb, M. A.; Frisch, M. J.; Schlegel, H. B. *Chem. Phys. Lett.* **1996**, *250*, 373−378.
(67) Rassolov, V. A.; Ratner, M. A.; Pople, J. A.; Redfern, P. C.; Curtiss, L. A. *J. Comput. Chem.* **2001**, *22*, 976−984.
(68) Abegg, P. W. *Mol. Phys.* **1975**, *30*, 579−596.
(69) Koseki, S.; Gordon, M. S.; Schmidt, M. W.; Matsunaga, N. *J. Phys. Chem.* **1995**, *99*, 12764−72.
(70) Marenich, A. V.; Cramer, C. J.; Truhlar, D. G. *J. Phys. Chem. B* **2009**, *113*, 6378−6396.
(71) German, E. D.; Efremenko, I.; Sheintuch, M. *J. Phys. Chem. A* **2001**, *105*, 11312−11326.
(72) Kuznetsov, A. M. *Charge Transfer in Physics, Chemistry and Biology*; Gordon & Breach: Reading, U.K., 1995.
(73) Kuznetsov, A. M. *Stochastic and Dynamic Views of Chemical Reaction Kinetics in Solutions*; Press politechnicues et universitaires romandes: Lausanne, Switzerland, 1999.